ELASTIC-PLASTIC FRACTURE MECHANICS ANALYSIS OF SMALL CRACKS

G. G. Trantina
H. G. deLorenzi
General Electric Corporate Research and Development
Schenectady, New York 12301

ABSTRACT

For many materials the fracture strength and fatigue lifetime is controlled by small cracks that can grow at sizes and applied stress levels which are below those predicted from data for long cracks. The objective of this paper is to describe how elastic-plastic fracture mechanics analysis can be used to interpret small crack behavior. The results of the elastic-plastic analysis indicate that deviations from LEFM begin at about 0.7 of the yield stress and that the trend of the small crack data can be predicted. The results of 3-D elastic-plastic analysis of a surface crack show a unique variation of the crack driving force along the crack front. This information is used to predict crack shapes during cyclic crack growth.

INTRODUCTION

Predictions of fracture strength and fatigue lifetimes of components fabricated with high strength materials require accurate representation of the crack driving force for small cracks. In addition, an understanding of short crack behavior is necessary for proper interpretation of test specimen behavior in fatigue and cyclic crack growth rate testing. For short cracks, crack geometry and material nonlinearity must be considered along with the three-dimensional nature of the surface crack. The objectives of this paper are to describe the fracture mechanics analysis procedure and the results of two- and three-dimensional finite element analysis of small surface cracks. The finite element analysis procedure involves the use of the deformation theory of plasticity, crack tip elements with blunting, and J-integral calculations by contour integrals and virtual crack extension. The results of elastic and elastic-plastic analysis of small surface cracks provide an indication of the limitations of linear elastic fracture mechanics (LEFM) and some techniques to modify the stress intensity factor for elastic-plastic conditions. The results of the analysis are used to interpret the fatigue growth threshold for small cracks and to predict crack growth shapes for small surface cracks.

Small crack behavior and the prediction of fatigue life has been reviewed recently by Hudak [1]. There are many observations that small cracks behave differently than large cracks. Small cracks can grow at sizes and applied stress levels which are below those predicted from threshold data for large cracks. Small cracks grow at faster rates than predicted from crack growth rate data for large cracks. Interpretation of the crack growth rate data from specimens with small cracks [2] and the prediction of growth of small intrinsic defects in specimens and components require proper representations of the crack tip stress field. The purpose of this paper is to demonstrate how

elastic-plastic fracture mechanics analysis can help to interpret the behavior of small cracks.

ANALYSIS TECHNIQUES

Plastic flow can be described by a total strain theory where the strain is given as a function of the actual stress state. The deformation theory of plasticity is a total strain theory and since the strains only depend on the final stresses, the strain state is independent of any particular loading path. In the uniaxial case the stress-strain law for this theory can be described by the Ramberg-Osgood law

$$\varepsilon/\varepsilon_y = \sigma/\sigma_y + \alpha(\sigma/\sigma_y)^n \qquad (1)$$

where ε_y is the yield strain, σ_y the yield stress ($\sigma_y = E\,\varepsilon_y$), α a material constant, and n the power hardening exponent. It is generally accepted that the deformation theory of plasticity does not model the path-dependent behavior of materials for radical departures from proportional loading (i.e., all stress components increase proportionally during loading). In applications where unloading and strong doviation from proportional loading is restricted to a small region of the structure, deformation theory is valid. For the analysis of small cracks described in this paper, unloading is not considered and thus deformation theory is used.

It has been shown that appropriate singularities can be induced in the isoparametric finite elements if the node points are arranged in an appropriate manner. Several authors have employed the 8-noded 2-D and 20-noded 3-D isoparametric elements in near tip modeling of 2- and 3-dimensional cracks. Henshell and Shaw [3] and Barsoum [4] pointed out that when the mid-side nodes in these elements are placed at the quarter-point position the elements will have a $1/\sqrt{r}$ singularity in the strain fields at the neighboring corner node, where r is the distance from the crack tip. This kind of element can, therefore, effectively be used around the crack tip in an elastic analysis. In the present investigation an elastic-plastic analysis was employed. The stress and strain singularity for a perfectly plastic material is 1/r and it has been shown by Barsoum [5] that the 8-noded 2-D and the 20-noded 3-D elements have the 1/r singularity when two corner nodes and a mid-side node are collapsed such that they initially are at the same location, but are allowed to separate when the elements deform.

For a power hardening material which is loaded into the plastic range, neither the $1/\sqrt{r}$ nor the 1/r singularity is theoretically the proper singularity to use. However, when collapsed elements are used at the crack tip in an elastic analysis, even the elastic stress intensity factors are determined very accurately. Since these elements lead to accurate results in the elastic and perfectly plastic limits, it is also believed that they will model the crack tip behavior accurately for a power hardening material in the entire elastic-plastic regime. These elements were therefore chosen for the crack

tip modeling in the finite element models. When the collapsed elements are used several nodes share the same location in the undeformed configuration. When the model is loaded, the crack tip elements will start to deform and the node points at the crack tip will start to separate. This will cause the crack tip to blunt and give a realistic modeling of the real crack tip behavior.

During the last few years, the J-integral has been used increasingly to characterize crack initiation and crack growth in the elastic-plastic regime. In the context of linear elasticity and deformation theory of plasticity, the J-integral simply denotes the energy released by a unit increase in crack area. The J-integral can be calculated by different techniques. In the 2-D analyses the J-integral was calculated from the path independent integral [6]

$$J = \int_C \left((W - \sigma_{11} \frac{\partial U_x}{\partial X} - \sigma_{21} \frac{\partial U_y}{\partial X}) dy + (\sigma_{12} \frac{\partial U_x}{\partial X} + \sigma_{22} \frac{\partial U_y}{\partial X}) dx \right) ds \qquad (2)$$

where W is the strain energy density, σ the stress tensor, and U the displacement vector. It has been shown [6] that when this integration is performed along a path around the crack tip, the integral is independent of the particular path both for elastic materials and for materials following the deformation theory of plasticity.

In the 3-D analyses the J-integral was calculated by the virtual crack extension method. With this technique the J-integral at a certain point on crack front is found from the local energy release rate at this point. J-integral can now be calculated by advancing the crack front a small ount at the point of interest as schematically shown in Figure 1a. This will increase the cracked area by the amount A. The J-integral is then defined as the total energy released by this crack advance divided by the area A. In a finite element model the local crack advance can be introduced by shifting the nodes near the crack tip as shown in Figure 1b. This leads to a virtual crack extension at that particular point and the change in energy in the surrounding elements can then be calculated. A detailed description of this method of calculating the J-integral is given in reference [7].

RESULTS AND DISCUSSION

Two-Dimensional Analysis

The 2-D analysis was performed to evaluate the effect of elastic-plastic material behavior on the stress intensity factor for a short crack. The Ramberg-Osgood representation of the stress-strain curve was used with a power hardening exponent (n) of 10. The finite element analysis of a tension-loaded double-edge crack plate was performed by using the mesh shown in Figure 2. This model, consisting of 8-noded isoparametric elements, represents one-quarter of the plate (Figure 3) and a crack length to plate width ratio (a/W) of 0.1. An a/W of 0.01 was also analyzed by adding 40 elements to the top and right side of the model. The results for these two cases were essentially the same indicating no significant effect of the plate width. Therefore, the

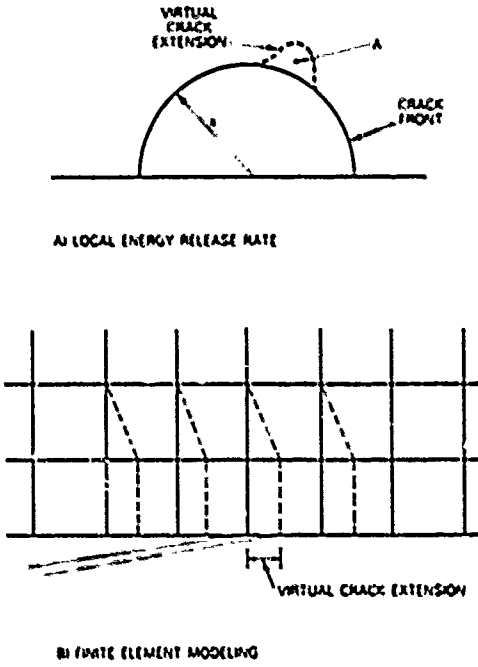

Figure 1. J-integral calculation by virtual crack extension.

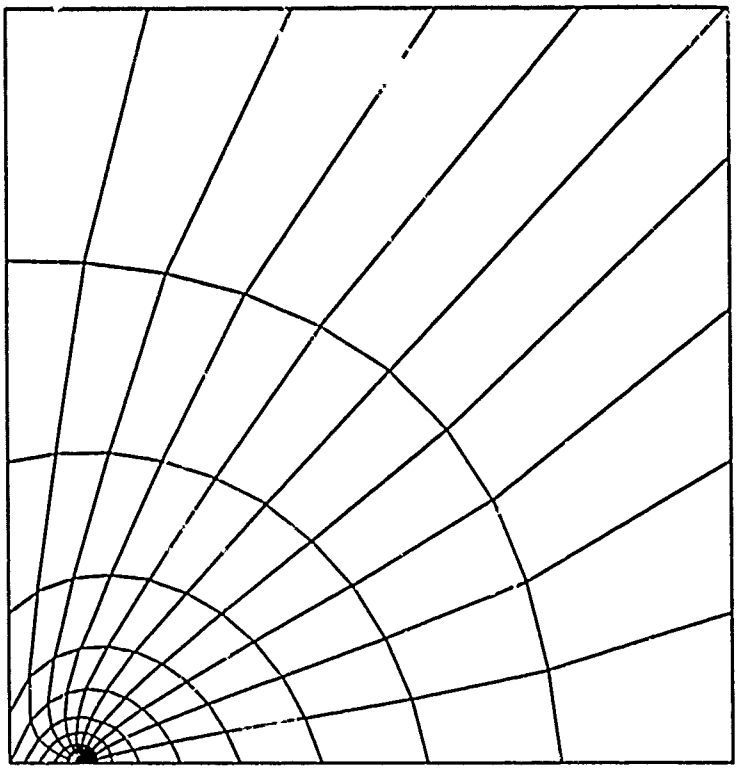

Figure 2. Finite element mesh for double-edge crack plate with a/W of 0.1.

crack behaves as a small crack in an infinite medium. The elastic-plastic analysis (deformation theory) was performed in 4 steps. The plastic zones (effective stress yield stress) for the last three steps of a plane strain analysis are shown in Figure 3. The development of the plastic zone follows the expected pattern for plane strain and does not seem to be affected by the free surface in this small displacement analysis.

The J-integral for a plane stress finite element analysis is computed by contour integrals and the stress intensity factor is computed as

$$K = \sqrt{EJ} \tag{3}$$

where E is the elastic modulus. These results are plotted in Figure 4 by normalizing the elastic stress intensity factor by

$$K = 1.12\ \sigma\sqrt{\pi a} \tag{4}$$

for an edge crack where σ is the applied stress and a is the crack length. Significant deviations from LEFM occur as σ/σ_Y increases with about a 5% deviation for $\sigma/\sigma_Y = 0.7$.

The J-integral can be estimated [8] from $J = J_e + J_p$ where J_e is the elastic part and J_p is the plastic part. The elastic J is computed by combining Eqs. (3) and (4) and adding a plastic zone size correction where

$$J_e = (1.12)^2\ (\sigma^2/E)\ \pi(a + r_Y) \tag{5}$$

and the plastic zone size correction for plane strain [9] is

$$r_Y = \frac{1}{6\pi}\ (K/\sigma_Y)^2 \tag{6}$$

The plastic J solution is given by

$$J_p = (1.12)^2\ f(n)\ \varepsilon_p\ \sigma\ a \tag{7}$$

where ε_p is the applied plastic strain and

$$f(n) = 3.85\ \sqrt{n}\ (1 - 1/n) + \pi/n \tag{8}$$

where $f(n) = 11.3$ for $n = 10$. With this estimation scheme the J-integral can be calculated and converted to K (Eq. (3)) to compare with the elastic solution and the finite element results (Figure 4). The estimated K's are very close to the values computed from the finite element results.

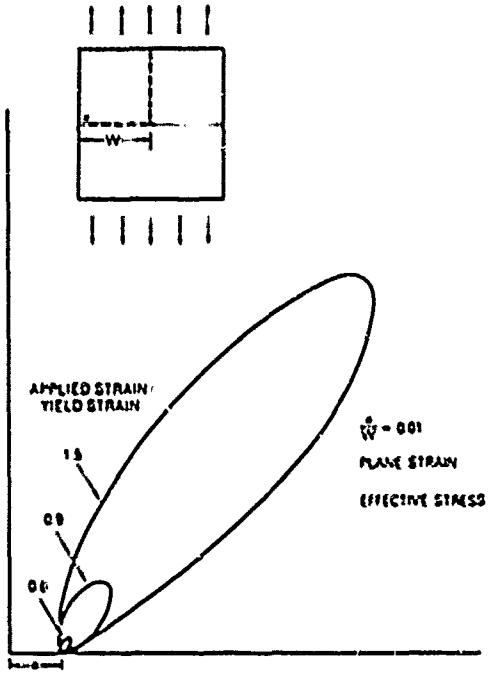

Figure 3. Plastic zone size as a function of applied strain.

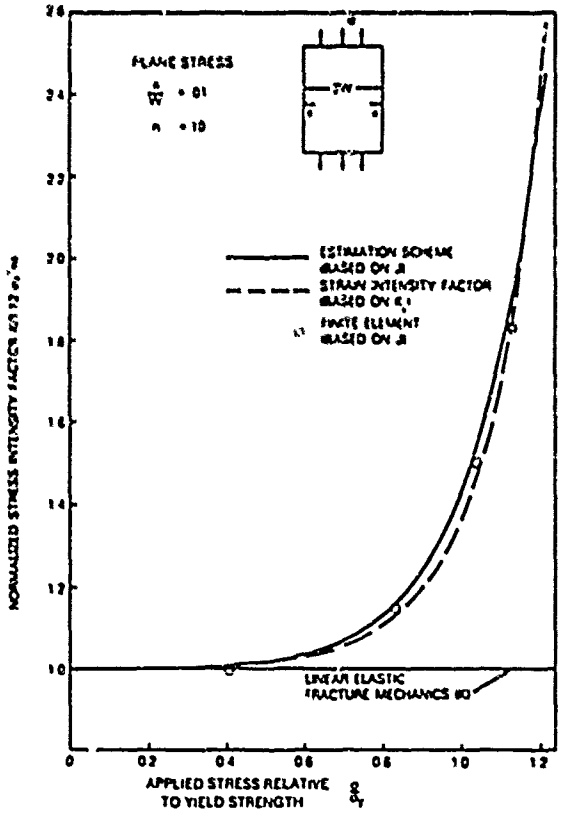

Figure 4. Effective stress intensity factors for double-edge crack plate.

Computing the stress intensity factor in terms of the applied strain rather than stress is a simple means of incorporating nonlinear effects in the crack tip parameter. This "strain intensity factor" is expressed as

$$K = 1.12\ E\ \varepsilon \sqrt{\pi(a + r_Y)} \tag{9}$$

where ε is the applied strain. The results with this simple method agree well with the finite element results as illustrated in Figure 4.

There has been an extensive amount of experimental data published concerning the cyclic crack growth rate behavior of small cracks. These experiments all indicate a deviation from LEFM behavior for small cracks. The data usually involves a plot of the cyclic stress ($\Delta\sigma$) required to propagate a crack versus the crack size. For large cracks the data follows the line predicted by LEFM ($\Delta\sigma\sqrt{a}$ = constant) while for short cracks $\Delta\sigma$ is less than predicted by LEFM. By normalizing the crack length by the plastic zone size (Eq. (6)), LEFM and the elastic-plastic fracture mechanics (EPFM) results in Figure 4 can be displayed as in Figure 5. The LEFM line is dependent only on the crack geometry (1.12) while the EPFM line is dependent on the power hardening exponent (n). Deviations between LEFM and EPFM begin when the applied stress is about 70% of the yield strength and the plastic zone size is about 10% of the crack length (Figure 5). This suggests that experimental data for the threshold of cyclic crack growth of small cracks should be treated with EPFM. A compilation of much of this data [10] is used here to demonstrate the use of EPFM to interpret the small crack behavior. The threshold value of the stress is normalized by the fatigue limit of a smooth specimen and plotted as a function of the crack length divided by the intrinsic crack length for the smooth specimen (Figure 6). The intrinsic crack length is defined by the LEFM relationship (Eq. (4)) where K is the threshold stress intensity factor and σ is the fatigue limit. The LEFM prediction fits the long crack data while for short cracks the threshold stress is considerably less than predicted (Figure 6). The EPFM prediction produced by using the results in Figure 4 and the assumption that the fatigue limit is 1.2 times the yield stress, fits the general trend of the data for long and short cracks. The data in Figure 6 represents a wide variety of steels, copper, and aluminum [10]. A power hardening exponent of 10, which is typical of many metals, was used for the EPFM prediction. However, a more precise prediction of the individual data points could probably be obtained by using the specific power hardening exponents for each of the materials.

Three-Dimensional Analysis

Many small surface cracks in test bars, crack growth rate specimens, and components are of a semicircular or semielliptical shape. These two-dimensional crack surfaces require a three-dimensional stress analysis. A 3-D finite element analysis of a small semicircular surface crack in a semi-infinite body has been performed. The actual 3-D mesh consists of a crack with a length equal to 0.1 of the radius of a half-cylinder which represents the semi-infinite body. The mesh has 340 20-noded isoparametric elements and

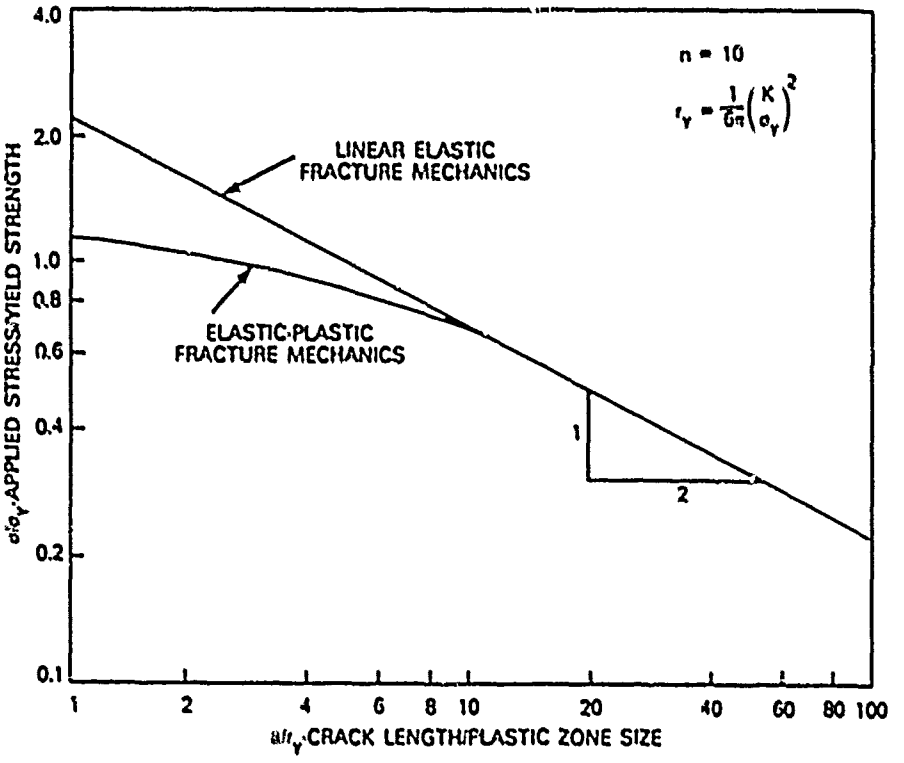

Figure 5. Difference in elastic-plastic and linear elastic fracture mechanics for small cracks.

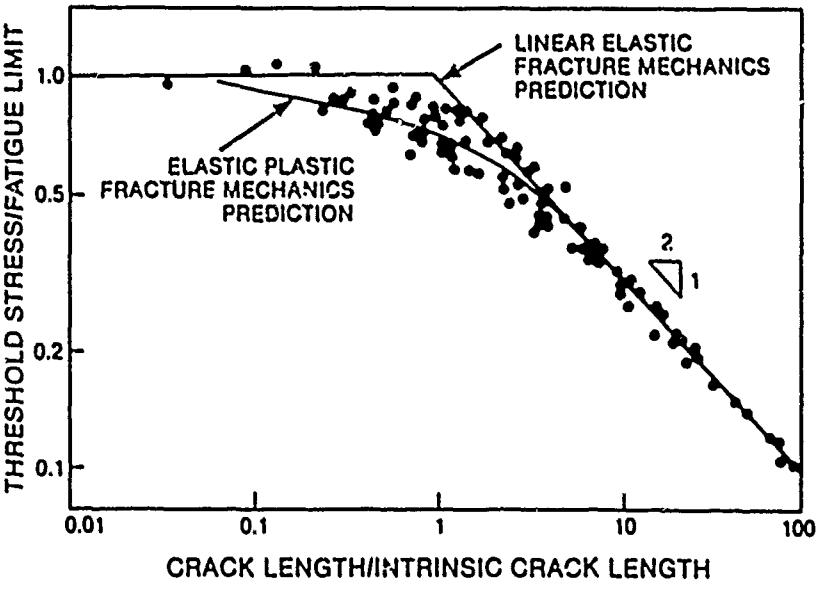

Figure 6. Threshold stress for cyclic crack growth data for various steels, copper, and aluminum [10].

1864 nodes. The known stress intensity factor for a semicircular surface crack is given by [11]

$$K = F(2/\pi)\ \sigma\sqrt{\pi a} \tag{10}$$

where σ is the stress applied perpendicular to the crack, a is the crack length, and F is a geometry factor. For a small surface crack the average value of F from other solutions [11] is 1.19 at the surface and 1.03 at the maximum depth point (90° from the surface). By using the virtual crack extension technique, the J-integral was calculated at 11 positions along the crack front. The J values were converted to K values by the relationships $K = \sqrt{JE/(1-\nu^2)}$ (Figure 7). These computed values at the surface and the maximum depth point were almost exactly the same as the average of the other solutions. This provides confidence in the finite element mesh and the computation of the J-integral for small 3-D surface cracks. These results for the elastic analysis show a smooth variation of F along the crack front. The small oscillations in the computed values (Figure 7) result from a piecewise linear model of the curved crack front.

An elastic-plastic analysis of the small, semicircular, surface crack was performed using the deformation theory of plasticity. One step to an applied stress of 0.7 of the yield stress was taken. The virtual crack extension technique was used to compute J and K as in the elastic analysis. The results show a unique variation of F along the crack front (Figure 7). For $\theta > 15°$ the stress intensity is beginning to increase due to elastic-plastic effects. This is consistent with the 2-D analysis. However, where the crack intersects the free surface ($\theta = 0$), the stress intensity has decreased. This effect is due to increased yielding at the free surface due to a lack of constraint. The region below the free surface, where there is plane strain constraint, carries a larger portion of the load. This variation in constraint along the crack front produces a plastic zone which is smaller in the interior than on the free surface.

An example of the use of this 3-D analysis in predicting crack shapes for cyclic crack growth is shown in Figure 8. The computed variation of K along the crack front is incorporated into a cyclic crack growth rate computation by using the power law crack growth rate relation. This expression can be integrated to compute the crack length as a function of cycles. One-half of four surface cracks is shown in Figure 8. In Figures 8a and 8b the initial surface crack is semicircular while in Figures 8c and 8d the depth-to-length ratio is 2.0 and 0.5, respectively. The crack shape is plotted when the crack has grown in the depth direction by an increment equal to 10% of the original depth (10% of the original surface length for Figure 8d). Figure 8a shows the growth of a crack for LEFM conditions while Figures 8b, c, and d include EPFM considerations as illustrated in Figure 7. The decreased amount of crack growth on the surface for the elastic-plastic conditions is a result of the decrease in the crack driving force on the surface and the increase in the crack driving force below the surface with increased plasticity (Figure 7). This prediction is consistent with experimental observations and empirical

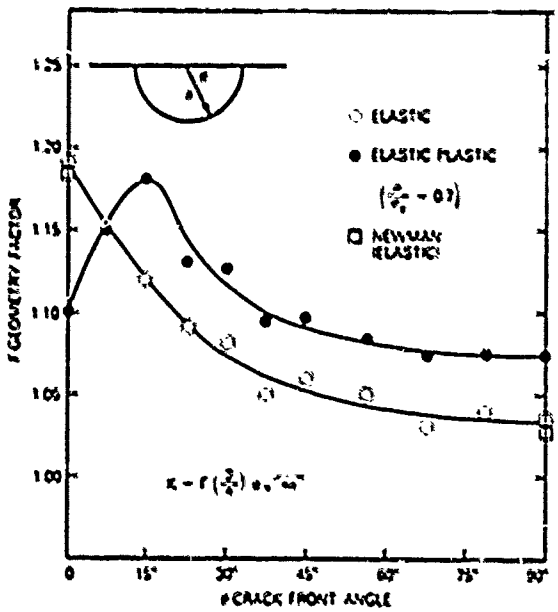

Figure 7. Stress intensity factor for semicircular surface crack for elastic and elastic-plastic loading.

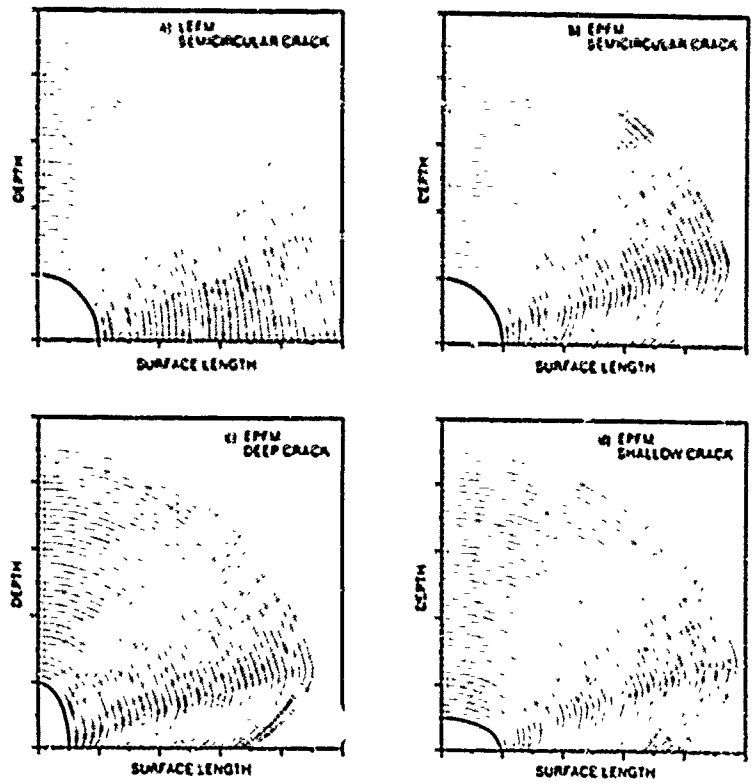

Figure 8. Crack shape predictions for cyclic crack growth.

adjustments to LEFM calculations [12]. In Figures 8c and d stress intensity factors for elliptical surface cracks [11] are combined with corrections for elastic-plastic conditions to show how deep and shallow cracks propagate to crack shapes that are nearly the same.

CONCLUSIONS

Predictions of fatigue lifetimes of components and test specimens and the interpretation of cyclic crack growth rate data require accurate representation of the crack driving force for small cracks. Results of two-dimensional analysis of an edge crack indicate that variations from LEFM begin at an applied stress of about 0.7 of the yield strength where the plastic zone size is about 0.1 of the crack length. Above this level an effective K can be calculated with the J-integral from finite element analysis or the J-integral estimation scheme or with a strain intensity factor. The trend of the small crack data for the threshold stress for cyclic crack growth can be predicted by EPFM techniques. The results of 3-D elastic-plastic analysis of a small surface crack show a unique variation of the crack driving force along the crack front with a decrease in the crack driving force at the surface and an increase in the crack driving force below the surface with increasing plasticity. This information was used to predict crack shapes for cyclic growth that are in general agreement with the observed trend of reduced crack growth on the surface.

REFERENCES

1. Hudak, S. J., Jr., "Small Crack Behavior and the Prediction of Fatigue Life," J. Eng. Mat. and Tech., v. 103, January 1981, 26-35.

2. Gangloff, R. P., "Electrical Potential Monitoring of Crack Formation and Subcritical Growth from Small Defects," Fat. of Eng. Mat., v. 4, no. 1, 1981, 15-33.

3. Henshell, R. D. and Shaw, K. G., "Crack Tip Elements are Unnecessary," Int. J. Num. Meth. Eng., v. 9, 1975, 495-507.

4. Barsoum, R. S., "On the Use of Isoparametric Finite Elements in Linear Fracture Mechanics," Int. J. Num. Meth. Eng., v. 10, 1976, 25-37.

5. Barsoum, R. S., "Triangular Quarter-Point Elements as Elastic and Perfectly Plastic Crack Tip Elements," Int. J. Num. Meth. Eng., v. 11, 1977, 85-98.

6. Rice, J. R., "A Path Independent Integral and the Approximate Analysis of Strain Concentration by Notches and Cracks," J. Appl. Mech., June 1968, 379.

7. deLorenzi, H. G., "Energy Release Rate Calculations by the Finite Element Method," to be published.

8. Shih, C. F. and Hutchinson, J. W., "Fully Plastic Solutions and Large-Scale Yielding Estimates for Plane Stress Crack Problems," J. Eng. Mat. and Tech., v. 98, October 1976, 289-295.

9. Irwin, G. R., "Plastic Zone Near a Crack and Fracture Toughness," Proceedings, Seventh Sagamore Conference, 1960, IV.63.

10. Tanaka, K., Nakai, Y., and Yamashita, M., "Fatigue Growth Threshold of Small Cracks," Int. J. Fract., v. 17, no. 5, October 1981, 519-533.

11. Newman, J. C., Jr., "A Review and Assessment of the Stress-Intensity Factors for Surface Cracks," in Part-Through Crack Fatigue Life Prediction, ASTM STP 687, J. B. Chang, Ed., American Society of Testing and Materials, 1979, 16-42.

12. Newman, J. C., Jr. and Raju, I. S., "An Empirical Stress Intensity Factor Equation for the Surface Crack," Eng. Fract. Mech., v. 15, no. 1-2, 1981, 185-192.